PROCEEDINGS OF SCIENCE

# Studying the robustness of quantum random walk search on Hypercube against phase errors in the traversing coin by semi-empirical methods

**Hristo Tonchev**[a*] **and Petar Danev**[a]

[a] *Institute of Nuclear Research and Nuclear Energy – Bulgarian Academy of Science, Boulevard "Tsarigradsko shose" № 72, Sofia, Bulgaria*

*E-mail:* htonchev@inrne.bas.bg, pdanev@inrne.bas.bg

In this work we obtain semi-empirical expressions for the probability to find solution of Quantum random walk search algorithm on hypercube when the traversing coin is constructed by generalized Householder reflection and an additional phase shift. Calculations are made for specific relations between coin phases (first from the reflection and second from the shift), that are obtained in our previous works. The quantum algorithm could be made more robust against phase errors, if an experimental implementation preserves those relations. The results from numerical simulations of quantum random walk search algorithm on hypercube are used to find an empirical formulas for algorithm's probability to find solution. Those formulas, obtained by fitting data to a suitable function, are used to make prognosis about the algorithm's robustness when dimension of the coin is too large to be simulated on classical computer. Here, we explicitly show all steps of the method used in the paper, while also discuss its advantages and limitations. The goal of this work is to help the experimental implementation of the quantum random walk search algorithm by giving evaluation of the algorithm's robustness and the obtained probability to find a solution when our design of the walking coin is used.

*11th International Conference of the Balkan Physical Union (BPU11),*
*28 August - 1 September 2022*
*Belgrade, Serbia*

[*]Speaker





PoS(BPU11)175

## 1. Introduction

One of the reason behind the huge interest in quantum computers is due to their ability to use the laws of quantum mechanics to compute variety of task faster than classical computers [1]. There are currently more than 60 quantum algorithms that are faster than their classical counterparts. Each of them have different speedup. Quantum computers can be used to factor numbers exponentially faster than best classical computers [1], can search unordered databases quadratically faster than a classical computer [1] [2] and can search ordered database approximately two times faster [3].

There are different kinds of quantum algorithms, based on the way they operate. One broad class of algorithms are those based on quantum random walk (QRW) [4]. Examples of such algorithms are quantum algorithm for verification of matrix products [5], quantum algorithm for calculating boolean formula [6], and quantum random walk search algorithm (QRWS) [2]. The latter can be used to search databases with arbitrary topology. Examples for some topologies on which the quantum random walk is studied are square grid [7], simplex [8], trees [9] and hypercube [10]. This algorithm was modified by many authors to improve in various ways the search on those structures.

Nowadays, many companies are trying to develop quantum computers. Few examples are Intel, Microsoft, IBM, IonQ, and Xanadu. They base their computers on different physical systems. Different implementations allow some operations to be performed more easily on some systems than on others. For example, in ion traps [11] and photonic quantum computers [12], the quantum gates can be constructed by decomposition to Householder reflections [13] and phase gates or by using just generalized Householder reflections **(**GHRs) [14]. The second method is quadratically faster than decomposition to Givens rotations [1]and can be done in case of operators with arbitrary dimension [14].

In our previous works [15] [16], we investigate the stability of QRWS on hypercube when the walk coin is constructed by GHR and an additional phase multiplier. We have studied probability to find solution for different relations between both phases (one from GHR and second from the multiplier): when the first one is constant (studied also in [17]), linear dependence between them, and two nonlinear connections. We have shown that the experimental implementation of those relations could lead to a significant increase in the quantum algorithm's robustness. The numerical results of the probability for those dependencies in the interval from 0 to $\pi$ for larger coin show behavior similar to sigmoid or Gauss function.

The Hill function is used in mathematical and computational biology [18]. Depending on parameter's values of the function, it can have the required form. The Hill function successfully describes reaction rate of many systems, for example binding of Oxigen to hemoglobin.

In this work we fit the probability of QRWS algorithm to find solution for the above mentioned functional dependencies with modified by us Hill function. With those fits we compute the modified Hill function's parameters, that allows us to make prognosis of the maximal probability to find solutions and robustness of the QRWS algorithm for given coin size and functional dependence between phases. Those results will be useful for experimental physicist that are implementing quantum random walk search algorithm, to chose the coin suitable to their experiments - depending on the difficulty of constructing it and desired robustness.

This work is organized as follows: in Section 2 a brief review of QRWS algorithm is given. Section 3 begins with description of our modification of the coin, definition for the robustness, and at the end gives the four different functional dependencies between phases as defined in[16]. Our modification of the Hill function is explained in Section 4. At Section 5 our method is explained in detail. The first subsection shows our fits for the probability of QRWS

algorithm to find a solution for different coin sizes and functional dependencies between coin angles. The standard deviation of those fits are evaluated and analyzed. The Hill function's parameters are extracted for all simulated coin sizes and, for each of those parameters, a secondary fit as a function of the coin size, is obtained (Section 5.2). In the next subsection we compare our fits of the of the probability to find solution based on the Hill function with simulations data. We also make extrapolations for the behavior of the probability for larger coin size. In the last subsection we use those fits with the modified Hill function to obtain prognoses for the maximal probability to find solution and the width of the stability range. Section 6 provides concluding remarks and discussions.



## 2. Discrete time quantum random walk search algorithm

Discrete time quantum random walk search algorithm DTQRWS is probabilistic quantum algorithm that finds element on graph that satisfies a given criteria. The algorithm is quadratically faster than the best known classical algorithms and can be used on graph with arbitrary topology. In this work we will focus on QRWS when it traverse a hypercube. Quantum circuit of the algorithm is shown on Fig. 1.

Algorithm uses three registers, first is control register that is used for control gates, it has only two states. The third one is the coin register. It corresponds to the number of edges coming from each node in the graph – it can have arbitrary dimension $m$ and it is determined by the topology. The second register is the register of nodes, and in the case of hypercube, its dimension is determined by the number of edges $2^m$.

The algorithm begins with modifying the initial state of node and coin registers from $|0\rangle$ to equal weight superposition. In case of registers of qubits it can be done by applying Hadamard gate on each qubit. Otherwise, when the register is made by qudits, the superposition can be obtained by applying the discrete Fourier transformation operator. Next, the algorithm continues with making the algorithm's iteration a fixed (no more, no less) number of times. The iteration itself consists of the following steps:

1) An oracle is applied on control and edge registers. It changes the state of the control register depending on whether the given node is a solution or not. The oracle should be made by a function that is able to recognize the solution when it is presented to it.

2) A walk coin is applied on the edge register (known also as coin register) on all states that are not solutions. It can be arbitrary unitary transformation with dimension equal to the coin register. However, the best coin that should be used depends on variety of factors including the topology and dimension of the walked object. In case of Hypercube, the most often is used the Grover's coin $C_0 = I - 2|\chi\rangle\langle\chi|$.

3) The marking coin is applied on all states that are solution. The best marking coin depends on the walk coin used. For hypercube and Grover walk coin, the best coin is $C_1 = -I$

4) The oracle is applied a second time.

5) The shift operator $S$ is applied on the registers of nodes and edges. Depending on the state of the edge register (the coins are applied on the edge register), it makes the transitions in the state of the register of nodes.

$$S = \sum_{i=0}^{2^m-1} \sum_{j=0}^{2^{2^m}-1} |i, j\rangle\langle i, j \overset{bitwise}{\oplus} i| \tag{1}$$

The algorithm ends with measurement of the node register. With certain probability the measured state will be the searched one. This probability have sinusoidal-like behavior that depends on the number of iterations made and on the coin used. However, in real systems there

are various effects that can interfere with the construction of the coin – from experimental setup imperfections to noisy environment. This is the reason why the robustness, against such errors is so important to be studied in detail.

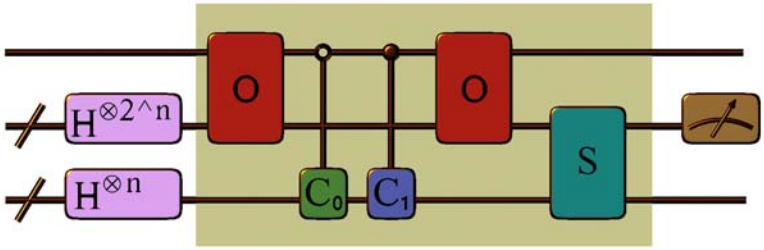


*Fig 1: Quantum circuit of the Quantum random walk search algorithm. The algorithm begins with applying discrete Fourier transform to each register. Next, a QRWS iteration is applied fixed number of times. Each iteration, represented with yellow rectangle, consists of the following gates: Oracle O, shift operator S, traversing $C_0$ and marking $C_1$ coins. The algorithm ends with measurement of the node register.*

## 3. Phase error of the traversing coin and our modification's robustness

The traversing coin changes the state of the coin register and thus determines the probability of going in either direction. Depending on the state of the coin register, the shift operator changes the node register' state.

The best way to construct a walk coin operator depends on the physical system, on which the algorithm is implemented. For example, for ion trap [11] and optical quantum computer [12], it is easy to implement a Householder reflection operator. If the walked graph is regular, all walk coins can be constructed by one GHR and one phase multiplier [14]:

$$C_0(\zeta,\varphi,n)=e^{i\varsigma}\left(I-(1-e^{i\varphi})|\chi\rangle\langle\chi|\right) \tag{2}$$

, where n is the dimension of the coin, the angles ζ and φ come from the phase multiplier and the generalized Householder respectively. In case of regular graph, $|\chi\rangle$ is equal weight superposition $|\chi\rangle=(1/\sqrt{m})\sum_{i=1}^{m}|i\rangle$ of all states i. So, the probability to find solution is function of three parameters:

$$P=P(\varphi,\zeta,m)=0.5-O(1/2^n)f(\zeta,\varphi) \tag{3}$$

A commonly used coin that in many cases gives the best result is the Grover coin. It can be obtained by Eq. (2) with:

$$\zeta=\varphi=\pi \tag{4}$$

However, in real physical system there are many imperfections. For example, variations in the laser field's phase and frequency, imprecise pulse shape, and others. Also there are many sources of noise that affect the physical system – such as random photons coming from an external medium that are absorbed. The probability of QRWS to find a solution strongly depends on the coin operator used, so all errors in it can lead to undesired effect. For example, if the noise changes phases to $\zeta=\varphi=0$, the coin $C_0$ becomes the identity operator and there is not walk at all.

This makes important the study of the quantum algorithm's implementation in the presence of noise. Here, we will discuss the case when there are errors in the phase. We say that algorithm is robust (against errors in the phase $\varphi$) if there is large interval $\Delta=(\varphi_{max}-\varepsilon^{-},\varphi_{max}+\varepsilon^{+})$

around its maximal value $\varphi_{max}$, where the probability to find solution is almost equal to its maximal value:

$$P\left(\varphi \in (\varphi_{max} - \varepsilon^{-}, \varphi_{max} + \varepsilon^{+}), \ldots\right) \simeq P_{max} = P(\varphi_{max}, \ldots) \tag{5}$$

In order to compare how different modifications of the coin are affected by phase errors, we define that one modification is more robust than other if the first one have larger interval of robustness Δ. In case of hypercube, when the coin size is larger than two, the points with largest probability to find solution are located in connected area [16]. A properly introduced functional dependencies between the phases $\zeta(\varphi)$ can be used to connect the points in this area with the highest probability to find solution. Those functions can differ for different coin size.

$$P(\varphi, \zeta, n) = P(\varphi, \zeta(\varphi), m = const) = P(\varphi) \tag{6}$$

They are symmetric about the line $\varphi = \pi$, and in this case $\varepsilon^{-} = \varepsilon^{+} = \varepsilon$. The probability to find solution as a function of the phase $P(\varphi)$, and its corresponding $\varepsilon$, for some relations $\zeta(\varphi)$ are obtained in [15]. Here we will show some of those relations, that will be used later in this study:
One angle is constant:

$$\zeta = \pi \tag{7}$$

The linear function with the largest $\varepsilon$:

$$\zeta = -2\varphi + 3\pi \tag{8}$$

Nonlinear function with large $\varepsilon$:

$$\zeta = -2\varphi + 3\pi - 1/(2\pi)\sin(2\varphi) \tag{9}$$

Suggested by machine learning value of $\alpha_{ML}$:

$$\zeta = -2\varphi + 3\pi + \alpha_{ML}\sin(2\varphi) \tag{10}$$

On Fig 2 is shown the probability to find solution P for QRWS on hypercube as a function of Householder phase φ. The left figure is for coin size 4, the right is for coin size 10. Each color and dashing represent different functional dependence between the two phases. Linear relations between phases Eq. (7, 8) are depicted by dot-dashed red and dashed teal curves accordingly. The nonlinear dependencies given by Eq. (9, 10) are too close and can not be distinguished on the figure.

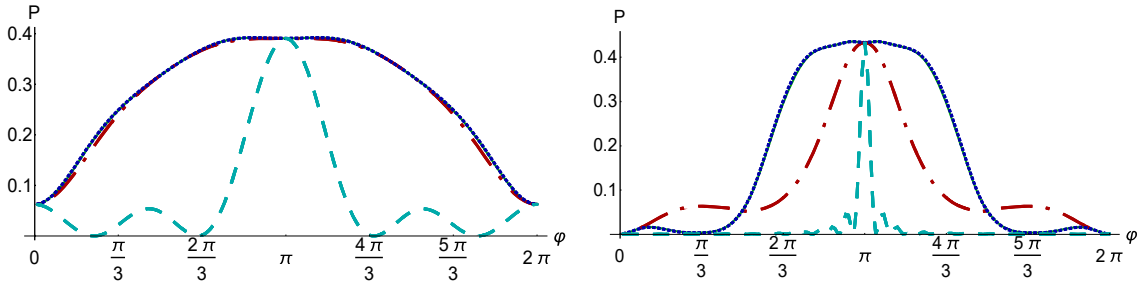


*Fig 2: Probability to find solution in implementation of QRWS algorithm, with walk coin parameters related as $\zeta(\varphi)$. The left picture is for coin size 4 and the right is for coin size 10. The red dot-dashed line corresponds to Eq (8), teal dashed - to Eq (7). The blue dotted and the green solid lines depict Eq (9) and Eq. (10). They give very close results, so its difficult to distinguish them without scaling the images.*

For all coin sizes between 4 and 12 (see [16]), the robustness of the quantum algorithm corresponding to those functions is ordered (from smallest to largest) as follows: Eqs. (7),(8),(9),

(10). In the interval between 0 and $2\pi$,the probability $P(\varphi,\zeta(\varphi),m)$ for all $\zeta(\varphi)$, is always similar to one of two functions:

1) Two Sigmoid-like functions. The one is a mirror copy of the other and both are connected together at the point $\varphi=\pi$.

2) Gaussian distribution with maximum at $\varphi=\pi$.

Both of those curves can be approximated by a modified Hill function.

## 4. Modification of Hill function

In biochemistry, mathematical and computational biology, there are variety of quantities of chemical processes, where the reaction are described by a different functions. Similar behavior to our results for $P(\varphi,\zeta(\varphi),m)$ can be seen for the reaction rate when one big molecule have different reaction centers and each of them can bound with a small molecule called inducer. When the binding events have an influence on each other (cooperative binding), that leads to nonlinear reaction rate. The current reaction rate depends of a variety of parameters - maximal reaction rate (b), free reacting centers (n), quantity of inducers (s) and complex formation ratio (k). This rate (H) is described by Hill function, that can be written as:

$$H(s,b,k,n)=\frac{bk^n}{s^n+k^n} \tag{11}$$

We use the Hill function coming from biochemistry and it should not be mistaken with the Hill equations in quantum mechanics, carrying the same name, that are solutions of the Hill differential equation – a second order differential equation for the periodic function f. The equation $u=u''-f(x)u$ is widely used in the quantum physics, for example in two level systems in quantum optics and in the condensed matter physics.

To be able to approximate the whole curves given by Eqs. (7,8,9,10) when $\varphi\in[0,2\pi]$ we modify Eq. (11) to:

$$W(x,b,k,n,w)=H(|x-w|,b,k,n)=\frac{bk^n}{|x-w|^n+k^n} \tag{12}$$

where in this case x is used as coordinate axis.

Here $s=|x-w|$ and is the same for x-w when x>0 and with x+w when x is less than zero. This means that this modulo mirrors the Hill function relative to the line $w=const$, and the parameter w corresponds to the center of the "bell shaped" function (see Fig 4 top center). The only condition for parameter w is to be real number, otherwise it interferes with the height (see Fig 4 down right)

The parameter b corresponds to the maximal height achieved at the point x=w (see Fig 4 top center). The value of b should be positive number, as the probability $W$ can not be negative.

The value of the parameter n corresponds to both: the curvature and slope of the curve (see Fig 4 top left). If n is not strictly positive, the modified Hill function is $W(x,b,k,0,w)=b/2$ for n=0 and $W(x,b,k,n<0)=b-W(x,b,k,|n|)$ for n<0 (see Fig 4 bottom left). The function $W(x,b,k,n<0)=b-W(x,b,k,n>0)$ have completely opposite behavior to $W(x,b,k,n>0,w)$, so where the first is ascending the second is descending. The first have maximum, where the second have maximum and vice versa. So, $W(x,b,k,n<0)$ describes completely different behavior and we can not use it in our fits. In our case n should be positive.

The parameter k is the translation of the mirrored curve (see Fig 4 top center). This effectively means that k corresponds to the width of the plateau. The width of the plateau depends on the value of $n$ (increases with n), but for high value of n it is approximately 2k and when $n\to\infty$, the plateau becomes equal to 2k. The height of the plateau is approximately $b$. The parameter k

should be positive, $k>0$. Otherwise, the function's behavior depends a lot on the value of n. When n is an odd number and $k<0$ the function W diverges (see Fig 4 bottom center). The divergence is coming from division by zero because parameters x, w, and k didn't obey $(x-w)^n \neq -k^n$. In case of negative k and non-integer $n$, W have a complex value, which is not physical. When n is even and $k<0$, the function W have the same result as if $k>0$. When $k=0$, the value of W is also 0.

On Fig 4 are shown examples for modified Hill functions with different parameters. Top figures shows the cases when parameters in the function obey the conditions discussed above, and bottom figure - when they don't.

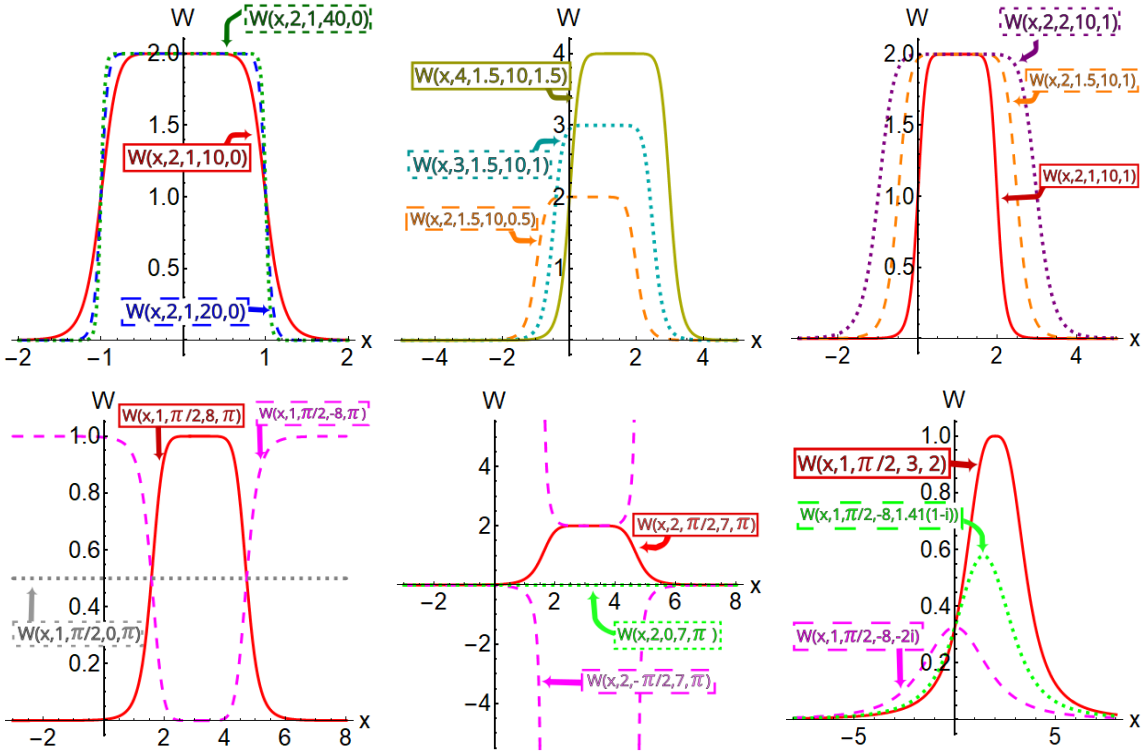


*Fig 4: Curves obtained by the modified Hill function W(x, b, k, n, w) with different parameters. Top left figure presents examples with different values of n. On the top right figure are shown examples with different values of w. The top center figure gives examples for different values of k. Bottom left figure shows examples when condition n>0 is not fulfilled. Bottom center figure gives examples when condition k>0 is not fulfilled. Bottom right figure gives examples for the cases when w is complex.*

In the next section, we will approximate $P(\varphi,\zeta(\varphi),m)$ by using the modified Hill function for different functional dependencies between the angles $\zeta(\varphi)$ and different coin sizes. Later, we will use those approximations to make prognosis for larger coin size that can not be simulated on the present computers.

## 5. Approximation of $P(\varphi,\zeta(\varphi),m)$ with modified Hill function

### 5.1 Fitting function $P(\varphi,\zeta(\varphi),m)$ for fixed coin size

In this section, we will find accurate semi-empirical expressions of the results for the probability of QRWS to find a solution by fitting the simulated data points with the modified Hill

function $W(x,b,k,n,w)$. In our work, the variable x corresponds to the angle φ. For all coin sizes, the functions described by equations (7,8,9,10), are symmetric relative to the axis $\varphi=\pi$. So, for all of them $w=\pi$. The values of all other parameters b, k, and n could change with the coin size m and described correlation between phases $\zeta(\varphi)$. The probability of QRWS to find solution expressed in the form of modified Hill function becomes:

$$W(\varphi,b,k,n)=W(\varphi,b,k,n,\pi)=\frac{b\,k^n}{|\varphi-\pi|^n+k^n} \tag{13}$$

The points, obtained by numerical simulations of QRWS algorithm, for all given functions $P(\varphi)$ (equations (7,8,9,10)) and coin sizes between 4 and 11 (showed in [16]), are fitted with modified Hill function (12). All fits have relatively small uncertainties as will be shown later in the work.

The quantum register of QRWS algoritm with coin size m have dimension that can be computed by the following formula $m2^{m+1}$. When we simulate the quantum algorithm, the PC's memory used to store the quantum register is proportional to register's size, so the memory requirements increase exponentially. The bigger vectors and operators also require more time to compute, in addition number iterations increase with the coin size as $k\sim\sqrt{2^{m-1}}$. As example, the simulations for coin sizes between 4 and 10 were performed on PC with the following characteristics: Intel I7 processor with 16 logical cores, 64 GB of RAM. For coin sizes 11 and 12 we use work station with 2 TB RAM, 20 computational cores AMD Ryzen 9 5900X. The work station was not able to simulate the quantum algorithm with coin size 13. In contrast to directly simulate the quantum algorithm, using approximation with Hill function will be much more simple. Here the task is reduced to calculations using a single formula without matrix calculus (see Section 5.2.). This allows to make predictions by using only PCs with characteristics similar to the mentioned above.

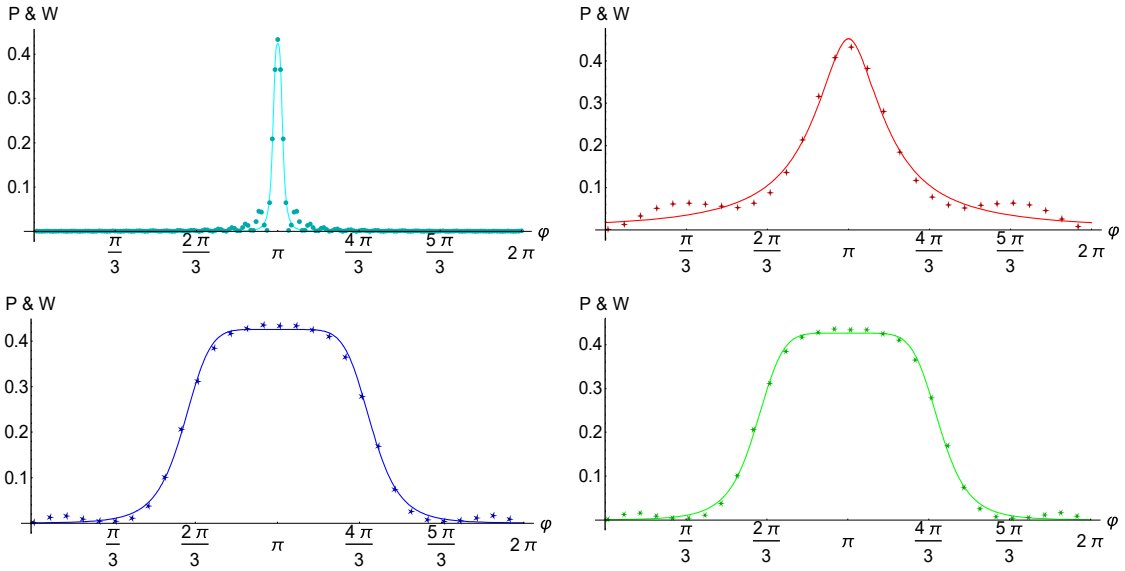


*Fig 5: Fitting the probability to find solution of QRWS for hypercube with modified Hill function. Traversing coin is with size 10 and is constructed by generalized Householder and additional phase. Each figure corresponds to different functional dependence. Top left is for Eq. (7), top right - (8), bottom left - (9), bottom right – (10). The solid curves represent the fitting curves, and with discrete symbols are shown the numerically computed data points.*

The numerical results for $P(\varphi,\zeta(\varphi),m)$, given by Eq. (6), for small coin size ( $m=2,3$ ) and all studied relations $\zeta(\varphi)$, have very different behavior from those with the larger coins. In order to make consistent fits for $m>3$, which are of primary interest to us, we exclude those cases from further consideration.

As an example, on Fig. 5 we show the fit of $P(\varphi,\zeta(\varphi),m)$in the case of coin size 10 for each of the functional dependencies between the angles $\varphi$ and $\zeta$. The figures corresponding to Eqs. (7,8,9,10) are shown on top left, top right, bottom left, and bottom right respectively. For each function, the fit is made by using 180 points, however to make the figures more clear, we show on them only 30 of the fitting data points (except for Eq. (7), where all of the 180 simulated points are plotted).

| Equation | b | k | n | σ |
|---|---|---|---|---|
| Eq. (7) | 0.423709 | 0.0659965 | 3.21164 | 0.00773994 |
| Eq. (8) | 0.452758 | 0.549574 | 1.85211 | 0.01788300 |
| Eq. (9) | 0.425852 | 1.19992 | 6.69816 | 0.00832803 |
| Eq. (10) | 0.426070 | 1.18997 | 6.48552 | 0.00836701 |

Table 1 *Modified Hill function parameters, resulted of fitting discrete time QRWS algorithm for hypercube when the coin register's size is 10. Each row corresponds to different functional dependence between phases and columns are for parameters b,k,n, and the standard deviation of the fit.*

The results of the fit for coin size 10 are shown on Table 1. Each row corresponds to different functional dependence between angles – equations (7), (8), (9) and (10) respectively. Each column represents different parameter in the modified Hill function (13) and the last column is for the standard deviation, defined as:

$$\sigma=\sqrt{\sum_{j=1}^{N}\frac{(W_j(\varphi,b,k,n)-P_j(\varphi,\zeta(\varphi),m))^2}{N-q}} \tag{14}$$

Here, N is the number of fitting data points, q – the number of fitting parameters (in our case 3 – $b,k,$ and $n$), $P_j(\varphi,\zeta(\varphi),m)$ is the $j^{th}$ point (i.e. at $\varphi=\varphi_j$) for the probability to find solution, simulated in our previous work [16]. Finally, $W_j(\varphi,b,k,n)$ is the $j^{th}$ fitted point for the probability $P(\varphi,\zeta(\varphi),m)$. The Table 1 shows that the standard deviation of the Eq. (8) fit (linear dependence) is much worse than the deviation of the other functions' fits.

We will investigate the behavior of $\sigma$ with the increase of the coin size. This will give us an estimate of how reliable will be the approximations based on a modified Hill function fits. In order to evaluate our method, we make prognosis for the standard deviation of the fits with increasing the coin size.

The values of $\sigma$ for all fits of equations (7), (8), (9), and (10) by modified Hill function are presented on Fig. 6. Points are for coin sizes between 4 and 11. All fits have relatively small standard deviation – less than 0.03. The best fits are for both nonlinear dependencies (Eq. (9), and Eq. (10)), and the worst is for Eq.(8). Here can be seen that the deviation decreases when coin size increase when the relation between phases $\zeta(\varphi)$ is defined by Eq. (7), (10) or (9). Eq. (7) leads to the lowest $\sigma$. This means that the modified Hill function (13) fits $P(\varphi,(\zeta(\varphi))_{by\,Eq.(7)},m)$ very well, and its prognosis is probably most reliable. In case of the relation given by Eq. (8), we see that the prognosis is that $\sigma$ slows it's increase and goes to a fixed value. This shows that prognosis made for this function is still useful, however less reliable than the predictions for the other functional dependencies. The fits corresponding to the nonlinear functions for $\zeta(\varphi)$ described by (9) and

(10), are most robust against the inaccuracies. The standard deviations of those fits decrease with increase of the coin size.

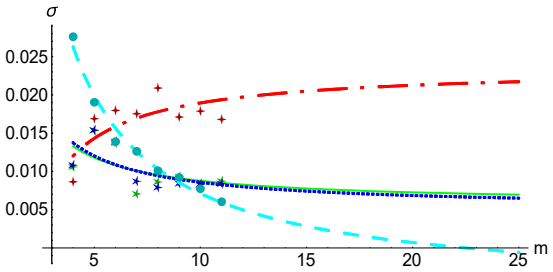


*Fig 6: Standard deviation of QRWS algorithm's fits when the walk coin is constructed according to Eqs.* (7), (8), (9), and (10). *The fitting expressions are found by fitting the numerical data points from our previous paper [16], to the modified Hill function. The red 4-pointed star labels the data corresponding to Eq.* (8) *and dot-dashed curve is the fit of those points. The teal circle corresponds to the results for Eq.* (7) *and dashed curve - to its fit. Similarly, the solid green line and 6-pointed star correspond to the fit and the numerical results coming from using Eq.* (10), *and the blue doted line and 5-pointed stars are for using Eq.* (9).

Once we are satisfied that this fit is good enough, we can continue with the next step. We will express the parameters b, k, and n in (13) as a simple functions of the coin size. Thus, the probability of the QRWS algorithm to find solution will become a function of only φ and m, for each relation $\zeta(\varphi)$investigated in the work.

## 5.2. Hill function for coin parameter relations of interest with respect to coin size

The results presented above, give us the basis to find more practical fitting expressions for all coin parameter relations (Eqs. (7), (8), (9) and (10)) studied in the previous section. In the new fitting formuale the probability to find solution depends only on two parameters – the phase $\varphi$ and the coin size m:

$$T_i(\varphi,m)=\frac{b_i(m)k_i(m)^{n_i(m)}}{|\varphi-\pi|^{n_i(m)}+k_i(m)^{n_i(m)}} \tag{15}$$

Here, the index $i=1,2,3,4$ corresponds to the different functional dependances between the traversing coin parameters $\varphi$ and $\zeta$ given by Eqs. (7), (8), (9), and (10). This is achieved by making secondary fits for the parameters b, k, and n (Eq. (12)) for all studied dimentions m, where the Hill function's properties were taken into account. The fits were done with simple two- and three-parameter expressions (see Table 2), so although we only have eight points ($m=4\div11$) for each parameter $b_i,k_i,n_i$ in Eq.(15), relatively accurate fits were achieved.

In Table 2 are given the fitting coefficients for all curves of the probability $T_i(\varphi,m), i=1,2,3,4$ corresponding to Eq. (15) and all functions $b_i(m),k_i(m),n_i(m)$ with their parameters.

As an example, on Fig. 8 are shown $T_i(\varphi,m)$ for both m=4 at top left and m=10 at top right. The blue five-pointed stars match very well the blue dashed curve, similarly the green six-pointed star coincide with the solid green curve. It can be seen that Eq.(15) fits really good the probability $P(\varphi,\zeta(\varphi),m)$ given by the functional dependences Eq. (9) and Eq. (10). The blue and green lines are very close to each other, that is why they cannot be distinguished on the figure. The teal dashed line fits the teal circles well too. The worst fit is for the dependence Eq. (8),

however around the high probability area the red dot dashed curve fits the points well enough. The results presented on Fig. 8 are similar to the original fits on Fig. 5. On the bottom line of Fig.8 are shown predictions for $P(\varphi,\zeta(\varphi),m)$ with the modified Hill functions for coin size m=15 (on the left side) and for coin size m=20 (on the right side).

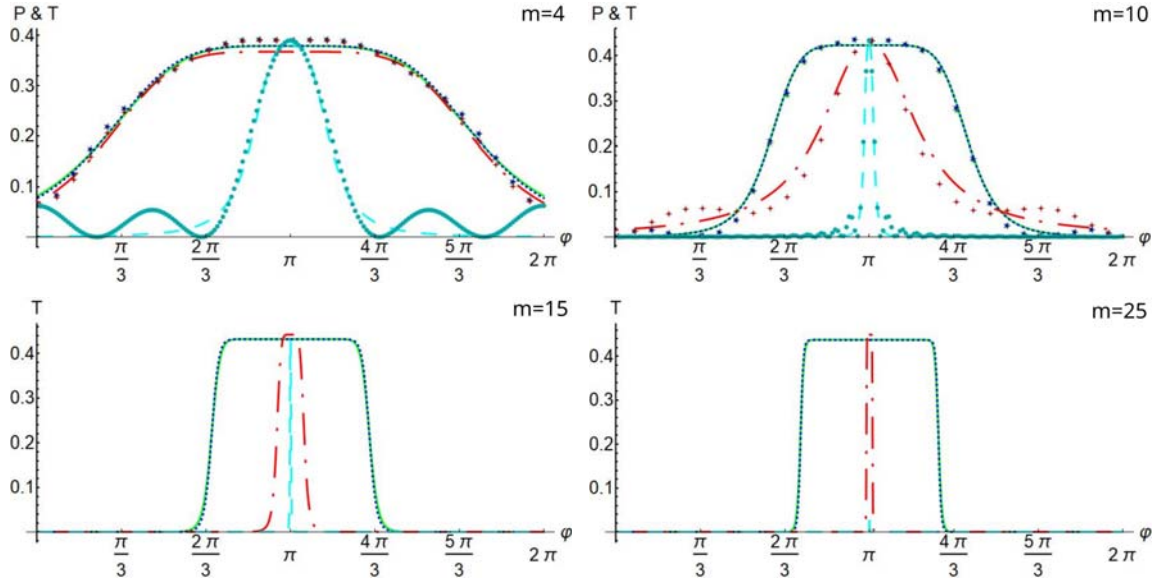


*Fig 8: (First row) A comparison between the numerically simulated data points for $P(\varphi,\zeta(\varphi),m)$ of QRWS for coin sizes 4 and 10 (where the teal circle, red four point star, blue five point star and green six point star correspond to the probabilities obtained from numerical simulation of Eqs.* (7), (8), (9) and (10)*) and our empirical expressions $T_i(\varphi,m)$, i=1,2,3,4 derived in this work, where the functions $b_i(\varphi),k_i(\varphi),n_i(\varphi)$ are taken from Table 2. The index i corresponds to different functional dependence Eqs. (7) showed as teal dashed line, (8) - red point-dashed line, (9) - blue dotted line and (10) - green solid line. (Second row) The prognoses of our fitting formulae (15) for the probability distribution $P(\varphi,\zeta(\varphi),m)$ for coin sizes 15 (left) and 20 (right).*

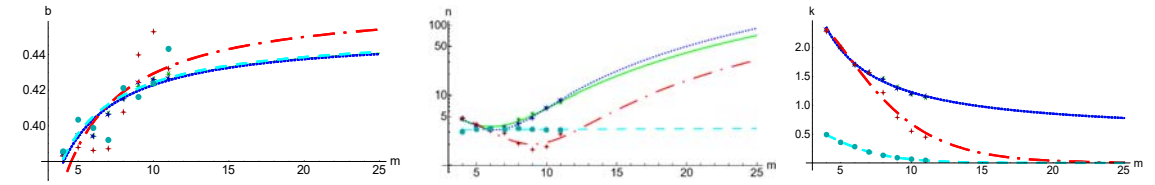


*Fig 7: On the picture are shown the functions $b_i(m)$, $n_i(m)$, and $k_i(m)$ that are taking part in Eq. (15) in interval $m\in[4,25]$. The left, the center, and the right correspond to $b_i(m)$ $n_i(m)$ $k_i(m)$ accordingly. The lines: teal dashed, red point-dashed, blue dotted, and green solid correspond to* (7), (8), (9) and (10*) respectively. The teal circle, the red four-pointed star, the blue five-pointed star, and the green six-pointed star corresponds to the results of numerical simulations of QRWS algorithm with functional dependence between phases corresponding to* (7), (8), (9), *and (*10*) accordingly.*

To show that our final expression given by Eq. (15), describes the behavior of the probability of QRWS algorithm to find solution as well as the initial fits (see Eq. (13) and Fig. 5),

we make Fig 9. There are presented the results for the parameters b, k, and n of the first fit, corresponding to each of the Eqs. (7), (8), (9), (10) and labeled with teal circle, red four-point star, blue five-point star and six-point star accordingly. The dashed teal line, red dash-doted line, blue doted line and solid green line show the fits of the functions $b_i(m)$, $k_i(m)$, and $n_i(m)$.

The computed points of the parameter b do not lay close enough to the fitting functions as one could expect. We believe, it comes from the nontrivial behavior of the functions $P(\varphi,\zeta(\varphi),m)$. For different coin size m and different relation $\zeta(\varphi)$, they show highly divergent behavior for the points around the maximum. On the other hand, the fits with Hill function average the points at the plateau. However, we want to make fits with as few parameters as possible and obtain truthful behavior of the parameter b. As this parameter corresponds to the maximum probability for QRWS to find a solution, and from theory $P_{max}(m\to\infty)=0.5$ [10], b should be positive and grow with increase of m to an asymptotic value at $m\to\infty$. Our fitting functions meet these criteria. All other fits of $k_i(m),n_i(m)$, with the parameters from Table 2, describe well the functions $W(\varphi,b,k,n)$ for all simulated coin dimensions m, and all relations $\zeta(\varphi)$. As can be seen on Fig. 7 that the functions $b_i(m),k_i(m)$, and $n_i(m)$ converge to a fixed point. This gives us reason to believe that those functions will not diverge for large coin sizes.

| Probability curve | Parameter | Fit function | Fit function's parameter values | | |
|---|---|---|---|---|---|
| | | | a | d | c |
| Eq.(7) $\zeta=const$ | $b_1$ | $a/m+d$ | - 0.2855 | 0.4528 | --- |
| | $k_1$ | $a\,m\,e^{d\,m}$ | 0.8822 | - 0.4954 | --- |
| | $n_1$ | $a\,m^2+dm+c$ | 0.0000 | 0.0080 | 3.195 |
| Eq.(8) $\alpha=0$ | $b_2$ | $a/m+d$ | - 0.4105 | 0.4704 | --- |
| | $k_2$ | $a\,m\,e^{d\,m}$ | 2.432 | - 0.3581 | --- |
| | $n_2$ | $a\,m^2+dm+c$ | 0.1162 | - 2.090 | 11.41 |
| Eq.(9) $\alpha=-1/(2\pi)$ | $b_3$ | $a/m+d$ | - 0.2897 | 0.4519 | --- |
| | $k_3$ | $a/m+d$ | 7.450 | 0.4817 | --- |
| | $n_3$ | $a\,m^2+dm+c$ | 0.2510 | - 3.194 | 13.41 |
| Eq.(10) $\alpha=\alpha_{ML}$ | $b_4$ | $a/m+d$ | - 0.2920 | 0.4524 | --- |
| | $k_4$ | $a/m+d$ | 7.442 | 0.4833 | --- |
| | $n_4$ | $a\,m^2+dm+c$ | 0.1898 | - 2.307 | 10.61 |

*Table 2: Functions $b_i(m),k_i(m),n_i(m)$ used in Eq. (15). The index i=1,2,3,4 corresponds to coin phase relations* (7), (8), (9), and (10*) respectively. "Fit function" shows the fitting function used. In the last three columns are given the parameters' values of those functions, that best fit the numerical results.*

## 5.3 Width of the stability range $\varepsilon$ and robustness of QRWS

The derived in this work empirical formulae $T_i(\varphi,m)$, allow us to investigate important quantities directly related to the robustness of the QRWS algorithm to inaccuracies in the Householder phase $\varphi$. Here, we will study the width of the high probability subrange in the angle $\varphi$ - this is the quantitative description of the robustness, defined in [16] as $\varepsilon$. This can be used to evaluate the acceptabe quantity of noise in the experiments, if the walk coin is constructed as is shown in this paper. The definition given above in Eq. (5) will be written in a more convenient form. The width $\varepsilon$ when the probability is larger than a particular value could be defined by:

$$T_i\left(\varphi \in (\varphi_{max}-\varepsilon, \varphi_{max}+\varepsilon)\right) \simeq \Omega T_{i,max}(\varphi_{max}, m) = \Omega T_{i,max}(m) \quad (16)$$

Here $\Omega$ is some value between zero and one, representing the percentage of the maximal probability wanted. The index i=1,2,3,4 corresponds to different relation between the coin phases $\zeta(\varphi)$ defined by Eqs. (7), (8), (9), and (10).To calculate the width of stability $\varepsilon$, the maximum probability to find solution $T_{i,max}(m)$ should be found first (see Eq. (16)).

The value of $T_{i,max}(m)$ for particular dependence between phase $\zeta(\varphi)$ can easily be calculated by Eq. (15) for the point $\varphi=\varphi_{max}=\pi$. The relations $b_i(m)$, $k_i(m)$, $n_i(m)$ (each i corresponds to particular $T_{i,max}(m)$) and their parameters are given in Table 2.

The prognosis for $T_{i,max}(m)$ for different coin sizes $m$ and dependencies between the coin phases is shown on Fig 9 left. The teal circle, red four-pointed star, blue five-pointed star and green six-pointed stars correspond to Eqs. (7), (8), (9), and (10) respectively. The curve corresponding to the phase relation given by Eq. (8) overestimates $T_{i,max}(m)$ the maximum probability. The reason behind the inaccurate value of $T_{i=2,max}(m)$ is the relatively low goodness of fit of the probability $P(\varphi, \zeta(\varphi), m)$ for $\zeta(\varphi)$ given by Eq. (8) as easily can be seen by higher standard deviation for the fits corresponding to Eq. (8) on Fig. 6. All other functional dependencies (Eqs. (7), (9), and (10)) show almost the same $T_{i,max}(m)$ as they should.

Having $T_{i,max}(m)$, we can substitute it in Eq. (15) and solve it for the particular percentage of maximal probability that is needed to get the values of $\varphi=\pi\pm\varepsilon$. From here $\varepsilon$ can be found easily.

The prognosis for $\varepsilon_i(m)$ when $\Omega=0.9$ is shown on Fig 9 right. The best is for Eq. (10), where errors in the coin phase greater than 20 degrees are acceptable, without disturbing the operation of the algorithm, even at large dimensions of the quantum register (m = 25). Slightly worse for the other non linear dependence Eq. (9). For small coin size Eq. (8) have high robustness but it decays fast with the increase of the coin size. Worst robustness is when Eq. (7) is used. In this case $\varepsilon_1(m)$ is small even for low dimension coin.

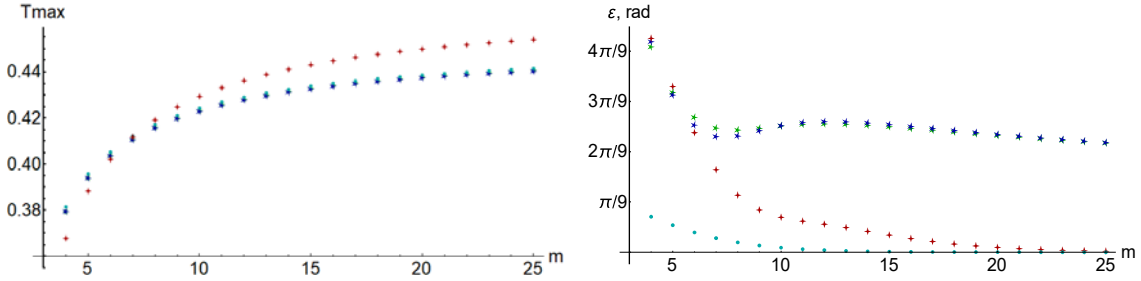


*Fig 9: The left figure shows a prediction for the maximum probability to find solution $T_{i,max}(m)$ as a function of the coin size. On right is shown he width of the stability range when the desired probability is at least $0.9\,T_{i,max}$. The teal circle, the red four-pointed star, the blue five-pointed star, and the green six-pointed stars corresponds to relations between phases according equations (7), (8), (9), and (10).*

From the figure it can be seen that the behavior of all $\varepsilon_i(m)$ is similar to the one predicted in [16]. Even the local minimum around coin size 6-7 is well described by our fitting formula (15), together with the decrease of $\varepsilon_i(m)$, as the size of the coin increases. The robustness of the QRWS algorithm corresponding to Eqs. (7), (8), (9), and (10), computed by approximations with the modified Hill function, is similar to the predicted stability of the algorithm by machine learning in our previous work [16]. The advantage of this work is that it gives approximate

formulae for calculation of the probability to find solution $T(\varphi,\zeta(\varphi),m)\simeq P(\varphi,\zeta(\varphi),m)$ and for the robustness of the studied coins.

By knowing the value of the width of stability for desired coin size for each functional dependence between phases, the experimental physicist can chose a coin that is optimal for the needs. They can do so by comparing desired robustness and difficulty in experimental implementation of the coin.

## 6. Conclusion

In this work we investigate the robustness of the Quantum random walk search algorithm on a hypercube with walk coin constructed by generalized Householder reflection and an additional phase multiplier. We make prognosis how the maximum probability to find solution and the width of robustness change with change of the coin size for specific functional dependence between the phases of the walk coin including: one constant phase, best linear connection between phases and two nonlinear dependencies. We were able to make prognoses for sizes above the values, that can be simulated on classical computer with reasonable amount of memory and time.

We make those predictions by first fitting the data from simulations of QRWS algorithm showed in our previous works, with modification of Hill function. The parameters of the obtained fitting expressions, were fitted themselves with simple few-parameter functions. As a result, formulae for the probability of QRWS algorithm to find a solution were derived as a function only of the coin's HR phase and the size of the coin register. This allows us to make prognosis for the maximal probability to find solution and the algorithm's robustness for arbitrary coin size. The reliability of the model obtained by those fits was also discussed here. We compare the goodness of fit for the different functional dependencies.

The end goal of this work is to give a practical and easy to use tool for experimental physicist that are realizing the high robustness modification of QRWS reviewed in this work, with different coin size and different relations between the phases. From all considered coins, the easiest to implement is when one of its angles is constant, but such coin requires very precise experimental setup and parameter control and also is the most sensitive to noise. The best linear dependence gives more robust performance for small coin size, however it decays fast with increasing the dimension of the coin. Both nonlinear functions show much better results even for large coin size, however they are more difficult to be implemented.

By knowing the prognosed value for the width of the stability range for particular coin size, together with the prognosis for the maximal probability to find solutions for a chosen correlation between phases, one can choose which dependence is best for particular implementation of the algorithm. The practical formulae derived in this work will allow for easier analysis, planning, and optimization of experimental realizations of the quantum random walk search algorithm with the modified walk coin, which we have shown can lead to improved robustness of the algorithm. The results presented here can be used to compare different experimental setups for running QRWS algorithm, depending on which coin relation can be implemented to achieve the desired robustness and expected gain. The fitting expression and the analyses presented in this work could be used as a basis for further more in-depth theoretical studies of the quantum random walk search algorithm's robustness.

## Acknowledgments

The work on this paper was supported by the Bulgarian National Science Fund under Grant KP-06-N58/5 / 12.02.2021.

## References:


[1] M. A. Nielsen and I. L. Chuang, *Quantum computation and quantum information*. Cambridge: Cambridge Univ. Press, 2007.

[2] N. Shenvi, J. Kempe, and K. B. Whaley, "Quantum random-walk search algorithm," *Phys Rev A*, vol. 67, no. 5, p. 052307, May 2003, doi: 10.1103/PhysRevA.67.052307.

[3] A. M. Childs, A. J. Landahl, and P. A. Parrilo, "Quantum algorithms for the ordered search problem via semidefinite programming," *Phys. Rev. A*, vol. 75, no. 3, p. 032335, Mar. 2007, doi: 10.1103/PhysRevA.75.032335.

[4] Y. Aharonov, L. Davidovich, and N. Zagury, "Quantum random walks," *Phys Rev A*, vol. 48, no. 2, pp. 1687–1690, Aug. 1993, doi: 10.1103/PhysRevA.48.1687.

[5] H. Buhrman and R. Špalek, "Quantum verification of matrix products," in *Proceedings of the seventeenth annual ACM-SIAM symposium on Discrete algorithm*, USA, 2006, pp. 880–889.

[6] A. Ambainis, A. M. Childs, B. W. Reichardt, R. Špalek, and S. Zhang, "Any AND-OR Formula of Size N Can Be Evaluated in Time $N^{1/2+o(1)}$ on a Quantum Computer," *SIAM J. Comput.*, vol. 39, no. 6, pp. 2513–2530, Jan. 2010, doi: 10.1137/080712167.

[7] A. Ambainis, J. Kempe, and A. Rivosh, "Coins Make Quantum Walks Faster," *ArXivquant-Ph0402107*, Feb. 2004, Accessed: Oct. 10, 2021. [Online]. Available: http://arxiv.org/abs/quant-ph/0402107

[8] L. Novo, S. Chakraborty, M. Mohseni, H. Neven, and Y. Omar, "Systematic Dimensionality Reduction for Quantum Walks: Optimal Spatial Search and Transport on Non-Regular Graphs," *Sci. Rep.*, vol. 5, no. 1, Art. no. 1, Sep. 2015, doi: 10.1038/srep13304.

[9] D. Koch and M. Hillery, "Finding paths in tree graphs with a quantum walk," *Phys. Rev. A*, vol. 97, no. 1, p. 012308, Jan. 2018, doi: 10.1103/PhysRevA.97.012308.

[10] V. Potoček, A. Gábris, T. Kiss, and I. Jex, "Optimized quantum random-walk search algorithms on the hypercube," *Phys Rev A*, vol. 79, no. 1, p. 012325, Jan. 2009, doi: 10.1103/PhysRevA.79.012325.

[11] P. A. Ivanov and N. V. Vitanov, "Synthesis of arbitrary unitary transformations of collective states of trapped ions by quantum Householder reflections," *Phys Rev A*, vol. 77, no. 1, p. 012335, Jan. 2008, doi: 10.1103/PhysRevA.77.012335.

[12] E. S. Kyoseva, D. G. Angelakis, and L. C. Kwek, "A single-interaction step implementation of a quantum search in coupled micro-cavities," *EPL*, vol. 89, no. 2, p. 20005, Jan. 2010, doi: 10.1209/0295-5075/89/20005.

[13] N. V. Vitanov, "Synthesis of arbitrary SU(3) transformations of atomic qutrits," *Phys Rev A*, vol. 85, no. 3, p. 032331, Mar. 2012, doi: 10.1103/PhysRevA.85.032331.

[14] P. A. Ivanov, E. S. Kyoseva, and N. V. Vitanov, "Engineering of arbitrary $\ textbackslashmathrm{U}(N)$ transformations by quantum Householder reflections," *Phys Rev A*, vol. 74, no. 2, p. 022323, Aug. 2006, doi: 10.1103/PhysRevA.74.022323.

[15] H. Tonchev and P. Danev, "Optimizing the walk coin in the quantum random walk search algorithm through machine learning," *ArXiv210508020 Quant-Ph*, Jul. 2021, Accessed: Oct. 10, 2021. [Online]. Available: http://arxiv.org/abs/2105.08020

[16] H. Tonchev and P. Danev, "High robustness quantum walk search algorithm with qudit Householder traversing coin, machine learning study," *ArXiv211110926 Phys. Physicsquant-Ph*, Nov. 2021, Accessed: Nov. 29, 2021. [Online]. Available: http://arxiv.org/abs/2111.10926

[17] Y.-C. Zhang, W.-S. Bao, X. Wang, and X.-Q. Fu, "Effects of systematic phase errors on optimized quantum random-walk search algorithm*," *Chin. Phys. B*, vol. 24, no. 6, p. 060304, Apr. 2015, doi: 10.1088/1674-1056/24/6/060304.

[18] U. Alon, *An Introduction to Systems Biology: Design Principles of Biological Circuits*. Accessed: Dec. 09, 2022. [Online]. Available: https://www.routledge.com/An-Introduction-to-Systems-Biology-Design-Principles-of-Biological-Circuits/Alon/p/book/9781439837177